

# Evolution of Thin Discs with Partial Accretion

K. Y. Ekşi

*Istanbul Technical University, Faculty of Arts and Letters, Physics Department, Maslak, 34469, Istanbul*  
*E-mail: ekşi@itu.edu.tr*

Released October 18, 2012

## ABSTRACT

The viscous evolution of a thin disc around a central object is considered. Such discs are described by self-similar solutions in which either all or none of the inflowing mass accretes. An approximate solution for the partial accretion regime is constructed by employing a prescription recently introduced for nonlinear heat conduction. The solution is compared with numerical simulations demonstrating that the approximate solution describes the intermediate asymptotic stage for partially accreting discs.

## 1 INTRODUCTION

Accretion of gaseous material onto a central object is a process at the heart of many diverse astrophysical phenomena, from quasars to the formation of planetary systems (Frank et al. 2002). In many cases accretion is via a geometrically thin disc (Shakura & Sunyaev 1973; Lynden-Bell & Pringle 1974).

The angular velocity of matter in the disc,  $\Omega$ , is keplerian ( $\Omega_K = \sqrt{GM_*/r^3}$  where  $G$  is the gravitational constant,  $M_*$  is the mass of the accreting object and  $r$  is the cylindrical radial distance from the center of the star) throughout the disc except in the narrow boundary layer where it matches to the angular velocity of the central object  $\Omega_*$  at the inner radius of the disc,  $r_{\text{in}}$ .

Accreting matter carries with it angular momentum which is acquired by the central object if it is rotating slower than the keplerian angular velocity at the inner radius of the disc (Pringle & Rees 1972). The rate of material angular momentum flux by accretion is  $\dot{L}_{\text{mat}} = \dot{M}r^2\Omega$  where  $\dot{M}$  is the accretion rate. Viscous stresses also lead to a flux of angular momentum  $\dot{L}_{\text{vis}} = 2\pi r^3\nu\Sigma d\Omega/dr$  where  $\nu$  is the kinematic turbulent viscosity and  $\Sigma$  is the surface mass density. In the steady state the mass accretion rate,  $\dot{M}$ , and the total angular momentum flux,  $\dot{L} = \dot{L}_{\text{mat}} + \dot{L}_{\text{vis}}$ , in the disc are integration constants. For a keplerian disc the angular momentum balance leads to

$$\nu\Sigma = \frac{1}{3\pi} \left( \dot{M} - \frac{\dot{L}}{\sqrt{GM_*r}} \right). \quad (1)$$

Usually one writes the total angular momentum flux in units of material stress for keplerian flow at the inner radius

$$\dot{L} \equiv \beta \dot{M} r_{\text{in}}^2 \Omega_K(r_{\text{in}}) \quad (2)$$

and the equation takes the more familiar form

$$\nu\Sigma = \frac{\dot{M}}{3\pi} \left( 1 - \beta \sqrt{\frac{r_{\text{in}}}{r}} \right). \quad (3)$$

Within the disc the viscous and the material torques can have different ratios though the total angular momentum flux is a constant determined by the fastness parameter  $\omega_* \equiv \Omega_*/\Omega_K(r_{\text{in}})$ . If the central object is rotating slowly, the angular velocity reaches a maximum value before matching the angular velocity of the star. At this point the viscous torque, as it depends on the radial angular velocity gradient, vanishes and the material torque is equal to the total angular momentum flux. If the boundary layer is narrow this allows one to estimate  $\beta \simeq 1$  for slowly rotating objects.

If the disc is truncated beyond the stellar radius e.g. by the strong magnetic dipole field of the star, it is possible without stellar break-up, that the angular velocity of the star is much greater than the keplerian angular velocity at the inner radius of the disc ( $\omega_* > 1$ ). In such cases the mass flux can diminish due to the centrifugal barrier (Illarionov & Sunyaev 1975) and the viscous torque is negative i.e. the angular momentum is transferred from the star to the disc ( $\beta < 0$ ). Sunyaev & Shakura (1977) gave a steady state solution for such “dead discs” in which mass flux (and so the material torque) is zero.

The steady state solutions of Shakura & Sunyaev (1973) and Sunyaev & Shakura (1977) have time-dependent counterparts as given by Pringle (1974). These are self-similar solutions and extend to the origin,  $r = 0$ . In the first solution the mass

accretion rate declines with a power-law in time while the angular momentum of the disc is constant ( $\dot{L} = 0$ ) (Cannizzo et al. 1990). In the second solution the mass of the disc is constant ( $\dot{M} = 0$ ) but angular momentum of the disc increases with the viscous torque at the inner boundary (Pringle 1991). These extreme boundary conditions and the extension of the disc to  $r = 0$  in the solution manifest the necessity that no length scale should exist in order that a self-similar solution can be found.

In reality, as the disc is not infinitely thin, matter vertically away from the disc plane can accrete even when matter is propelled at the midplane. Thus there should be a transition stage between these full accretion and full propeller stages during which the central object will accrete a fraction of the inflowing material (Menou et al. 1999; Ekşi & Kutlu 2010; Romanova et al. 2004; Ustyugova et al. 2006) depending on the fastness parameter. Furthermore, it is expected that an episodic accretion stage (Spruit & Taam 1993; D’Angelo & Spruit 2011, 2012) will be realized near the transition stage separating the full accretion and full propeller stages. Such a stage can not be described as a succession of steady states as  $\dot{M}$  is an integration constant and hence whatever the accretion rate in the disc should be the rate of accretion onto the star. The self-similar solutions because they correspond to extreme boundary conditions, either  $\dot{L} = 0$  or  $\dot{M} = 0$ , also can not accommodate the continuum of angular momentum flux per mass accretion rate,  $\dot{L}/\dot{M}$ , to be realized in the continuous transition between the full propeller and full accretor stages.

In this work we construct an approximate self-similar time dependent solution via a prescription recently used by Ekşi (2009) for self-similar evolution of temperature distribution in a semi-infinite rod with partial heat insulation at one boundary. In the next section disc structure equations and the self-similar solutions of Pringle (1974) is reviewed. In §3 the “nonlinear superposition” method of Ekşi (2009) is applied to these solutions to construct a self-similar approximate solution with arbitrary values of  $\beta$ . In §4 we demonstrate the accuracy of the approximate analytical solution by comparing it with numerical results. In the final section we discuss some implications for neutron star soft X-ray transients.

## 2 EVOLUTION OF THE DISC

We consider the evolution of a non-self-gravitating viscous thin disc in the gravitational field of a central mass  $M_*$ .

### 2.1 Thin Disc Equations

The conservation of mass in cylindrical coordinates reads

$$\frac{\partial \Sigma}{\partial t} = \frac{1}{2\pi r} \frac{\partial \dot{M}}{\partial r} \quad (4)$$

where  $\Sigma$  is the surface mass density and

$$\dot{M} = 2\pi r \Sigma (-v_r) \quad (5)$$

is the mass flow rate,  $v_r$  being the radial velocity. The conservation of angular momentum reads

$$\frac{\partial}{\partial t} (r^2 \Omega \Sigma) = \frac{1}{2\pi r} \frac{\partial \dot{L}}{\partial r}. \quad (6)$$

where  $\Omega$  is the angular velocity of the fluid and

$$\dot{L} = \dot{M} r^2 \Omega + 2\pi r^3 \nu \Sigma \frac{\partial \Omega}{\partial r} \quad (7)$$

is the angular momentum flux (torque). The first term is the material torque and the second term is the viscous torque where  $\nu$  is the turbulent kinematic viscosity.

The form of the conservation equations (4) and (6) make it clear that in the steady state the accretion rate  $\dot{M}$  and angular momentum flux  $\dot{L}$  are two integrals of motion. Assuming the matter in the disc is in Keplerian orbits,  $\Omega = \Omega_K$  where  $\Omega_K \equiv \sqrt{GM_*/r^3}$ , Equation (6) with the help of Equation (4) reduces to

$$\dot{M} = 6\pi r^{1/2} \frac{\partial}{\partial r} \left( \nu \Sigma r^{1/2} \right) \quad (8)$$

This then can be plugged into Equation (4) to give the diffusion equation

$$\frac{\partial \Sigma}{\partial t} = \frac{3}{r} \frac{\partial}{\partial r} \left[ r^{1/2} \frac{\partial}{\partial r} \left( \nu \Sigma r^{1/2} \right) \right] \quad (9)$$

for the evolution of the surface mass density. The equation is linear if  $\nu$  does not depend on  $\Sigma$ . In general the viscosity depends on  $\Sigma$  and the equation is nonlinear.

The rest of the disc structure equations are as follows (Frank et al. 2002): We employ Shakura & Sunyaev (1973) turbulent viscosity prescription  $\nu = \alpha c_s H$  where  $\alpha \sim 0.01 - 0.1$  is the dimensionless viscosity parameter,  $c_s = \sqrt{P/\rho}$  is the sound speed,  $H = c_s/\Omega_K$  is the disc scale height and  $P$  is the pressure. The density is then given by  $\rho = \Sigma/H$ . Assuming the heat produced by viscous processes are radiated locally, the energy balance can be written as  $4\sigma_{\text{SB}} T^4/3\Sigma\kappa = \frac{9}{8}\nu\Sigma\Omega_K^2$  where  $T$  is the temperature at the disc mid plane and  $\kappa$  is the Rosseland mean opacity. These equations are then supported by the

equation of state  $P = P(\rho, T)$  and a prescription for the opacity  $\kappa = \kappa(\rho, T)$ . The pressure has contributions from both the gas pressure,  $P_{\text{gas}} = \rho k_{\text{B}} T / \bar{\mu} m_{\text{p}}$  where  $\bar{\mu}$  is the mean molecular weight, and radiation pressure  $P_{\text{rad}} = 4\sigma_{\text{SB}} T^4 / 3c$ . We assume the gas pressure dominates the radiation pressure throughout the disc. Opacity is in general of the form  $\kappa = \kappa_0 \rho^a T^b$  where  $\kappa_0$ ,  $a$  and  $b$  are constants depending on the dominating opacity regime (e.g.  $a = b = 0$  and  $\kappa_0 = 0.4 \text{ cm}^2 \text{ g}^{-1}$  for electron scattering). These algebraic disc structure equations can be solved among themselves first to obtain viscosity (and other variables) in terms of  $r$  and  $\Sigma$  in the form

$$\nu = Cr^p \Sigma^q \quad (10)$$

where  $C$ ,  $p$  and  $q$  are constants determined by the dominant opacity regime and pressure (see e.g. Cannizzo et al. (1990); Ertan et al. (2009)). This then can be plugged in the diffusion equation (9) to obtain an equation containing  $\Sigma$  only. For discs in which gas pressure and electron scattering opacity dominates  $p = 1$  and  $q = 2/3$  (Cannizzo et al. 1990). In comparing the analytical solutions with the numerical solutions we assume this regime to prevail throughout the disc though it is well known that different opacity and pressure regimes prevail at different locations of the disc depending on temperature  $T(r, t)$ .

## 2.2 Pringle Solutions

In order to apply self-similarity methods we render the equation dimensionless via  $R = r/r_0$ ,  $\tau = t/t_0$  and  $\sigma = \Sigma/\Sigma_0$ , and define  $\nu_0 = Cr_0^p \Sigma_0^q$ . Choosing  $t_0 = 4r_0^2/3\nu_0$  we obtain

$$\frac{\partial \sigma}{\partial \tau} = \frac{4}{R} \frac{\partial}{\partial R} \left[ R^{1/2} \frac{\partial}{\partial R} \left( R^{p+1/2} \sigma^{q+1} \right) \right]. \quad (11)$$

Self-similarity methods (Zel'Dovich & Raizer 1967) provide two solutions of this equation as first found by Pringle (1974) (see also Lynden-Bell & Pringle (1974); Tanaka (2011); Mineshige (1991); Mineshige et al. (1993)). The first solution which we call the ‘‘full accretor solution’’, for reasons to be explained in the following subsection, is

$$\sigma(R, \tau) = \begin{cases} (1 + \tau)^{-\frac{5}{5q-2p+4}} \left( R(1 + \tau)^{-\frac{2}{5q-2p+4}} \right)^{-\frac{p}{q+1}} \left[ 1 - k_{p,q} \left( R(1 + \tau)^{-\frac{2}{5q-2p+4}} \right)^{2-\frac{p}{q+1}} \right]^{1/q}, & \text{if } q \neq 0, \\ (1 + \tau)^{\frac{5-2p}{2(p-2)}} R^{-p} \exp\left(-\frac{R^{2-p}}{4(p-2)^2(1+\tau)}\right), & \text{if } q = 0 \end{cases} \quad (12)$$

where

$$k_{p,q} = \frac{q}{(4q - 2p + 4)(5q - 2p + 4)}. \quad (13)$$

The second solution which we call the ‘‘full propeller solution’’ is

$$\sigma(R, \tau) = \begin{cases} (1 + \tau)^{-\frac{4}{4q-2p+4}} \left( R(1 + \tau)^{-\frac{2}{4q-2p+4}} \right)^{-\frac{p+1/2}{q+1}} \left[ 1 - k_{p,q} \left( R(1 + \tau)^{-\frac{2}{4q-2p+4}} \right)^{\frac{5}{2}-\frac{p+1/2}{q+1}} \right]^{1/q}, & \text{if } q \neq 0, \\ (1 + \tau)^{\frac{3-2p}{2(p-2)}} R^{-p-\frac{1}{2}} \exp\left(-\frac{R^{2-p}}{4(p-2)^2(1+\tau)}\right), & \text{if } q = 0. \end{cases} \quad (14)$$

Note that Equation (9) is symmetric under translations in time and hence the solutions can also be shifted in time. We have exploited this to write the original solutions shifted as  $\tau \rightarrow \tau + 1$ . Note also that the solutions for the linear cases ( $q = 0$ ) can be found from the nonlinear cases by referring  $\lim_{q \rightarrow 0} (1 + Aq)^{1/q} = \exp A$ . In the linear solutions the  $p = 2$  case should be handled separately as is done by Pringle (1974). We do not write the solution for this case as it would not contribute to the main motivation of the paper.

In the non-dimensionalization process we have employed four quantities,  $\Sigma_0$ ,  $r_0$ ,  $t_0$  and  $\nu_0$ , related by two equations  $\nu_0 = Cr_0^p \Sigma_0^q$  and  $t_0 = 4r_0^2/3\nu_0$ . This means we are free to attribute any value for two of the variables e.g.  $\Sigma_0$  and  $r_0$ . We fix these two quantities in terms of the initial mass and angular momentum of the disc (see Ertan et al. 2009).

## 2.3 Properties of solutions

The Pringle solutions given in Equations (12) and (14) describe the evolution of thin discs with free outer boundaries and thus are more appropriate for discs that are not truncated e.g. by tidal torques. The physical meaning of the first solution (full accretor) was clarified by Cannizzo et al. (1990) who modeled the evolution of a disc formed by tidally disrupted star around a supermassive black hole. Soon afterwards Pringle (1991) used the second solution for describing the evolution of circumbinary discs. Mineshige (1991) used the first solution for the evolution of dwarf nova discs. Mineshige et al. (1993) used it for the evolution of the putative disc around the neutron star assumed to form in SN 87A. Since the original work of Chatterjee et al. (2000) the first solution has been employed for describing fallback discs (e.g. Perna et al. 2000; Ertan et al. 2009) around young neutron stars. Ekşi & Alpar (2003) employed both two solutions, the first one for the accretion and the second one for the propeller stages of the system, respectively.

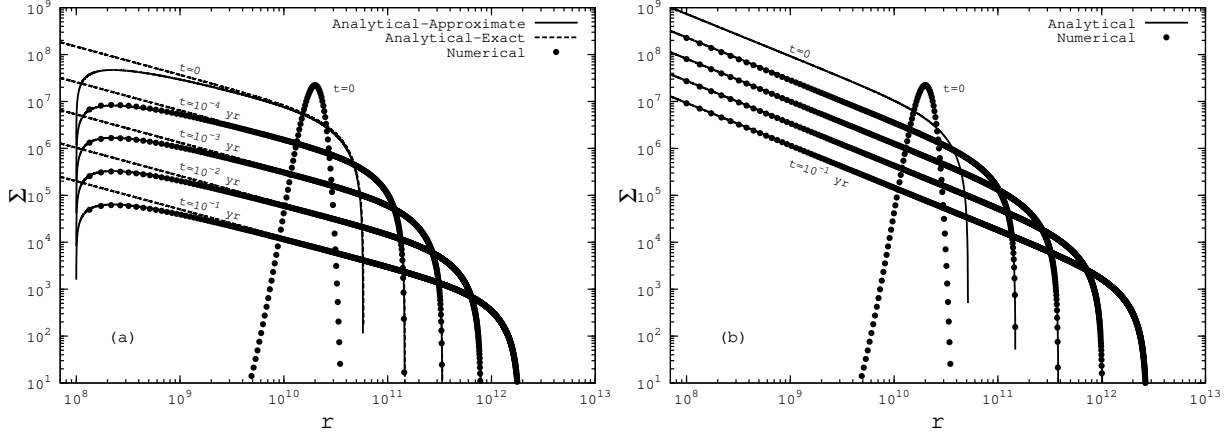


**Figure 1.** Comparison of the analytical and numerical solutions of the diffusion equation (9) for the full accretor (panel a) and full propeller (panel b) inner boundary conditions,  $\Sigma = 0$  and  $\partial(r^{1/2}\nu\Sigma)/\partial r = 0$  at  $r = r_{\text{in}}$ , respectively. The filled circles show the numerical solution which starts from a Gaussian surface density distribution. On the left panel the solid line shows the approximate analytical solution given in Equation (30) for  $n = 1$ . The dashed line shows the exact Pringle solution given in Equation (19).

The properties of the solutions given in Equations (12) and (14) are understood and classified in terms of the time evolution they result for the mass

$$M_d = \int_0^{r_{\text{out}}} \Sigma \cdot 2\pi r dr \quad (15)$$

and the angular momentum

$$L_d = \int_0^{r_{\text{out}}} r^2 \Omega_K \Sigma \cdot 2\pi r dr, \quad (16)$$

of the disc. Here  $r_{\text{out}}$  is the freely expanding outer boundary of the disc defined as the location where the square bracket terms in the solutions given in Equations (12) and (14) vanish. The lower limit of the integrals is zero as the solutions extend to the origin. A real disc will have a finite inner radius and so the integrals then can provide the correct parameters as long as this inner radius is much smaller than the outer radius.

### 2.3.1 Full Accretor Solution

According to the first solution given in Equation (12), the outer boundary of the disc evolves as  $r_{\text{out}} \propto (1 + \tau)^{2/(5q-2p+4)}$ . The mass of the disc decays with  $M_d \propto (1 + \tau)^{-1/(5q-2p+4)}$  so that mass flux out of the disc is

$$\dot{M}_d = \dot{M}_0 (1 + \tau)^{-1 - \frac{1}{5q-2p+4}}, \quad (17)$$

where  $\dot{M}_0 \equiv 3\pi\nu_0\Sigma_0$  is the initial mass flow rate in the disc. In this solution the angular momentum of the disc is constant ( $\dot{L}_d = 0$ ): the outer radius of the disc expands at the exact rate to take up the angular momentum lost from the inner disc by the accreting mass.

Cannizzo et al. (1990) showed that this solution describes the evolution of the disc with the absorbing inner boundary condition  $\Sigma(r_{\text{in}}, t) = 0$  at the inner radius of the disc,  $r_{\text{in}}$ . In this solution  $\sigma \propto R^{-p/(q+1)}$  for most part of the disc except near the outer boundary which the terms in square brackets handle. As shown in the next section this also is the radial profile in the steady-state counterpart (Shakura & Sunyaev 1973) away from the inner boundary of the disc. The self-similar solutions are thus said to describe a quasi-static regime i.e. successive steady-states with decreasing accretion rates (Pringle 1974; Chan et al. 2005). According to this solution the disc extends to the origin and  $\sigma$  blows out there. In the numerical solution  $\sigma$  overturns trying to match the inner boundary condition. As first remarked by Ertan et al. (2009) the time shifted solutions where  $r_0$  and  $\Sigma_0$  are fixed by referring to the initial mass and angular momentum in the disc gives a better match to the numerical solution. The numerical solution settles to the self-similar solution in a few diffusive timescales. As such self-similar solutions describe the intermediate asymptotic regime (Barenblatt 1996) as they prevail after the initial conditions are forgotten and before the disc vanishes completely.

### 2.3.2 Full Propeller Solution

According to second solution given in Equation (14) but shifted in time the outer radius evolves as  $r_{\text{out}} \propto (1 + \tau)^{2/(4q-2p+4)}$ . The mass of the disc is constant ( $\dot{M}_d = 0$ ) and the angular momentum of the disc increases as  $L_d \propto (1 + \tau)^{1/(4q-2p+4)}$  so that

the angular momentum flux evolves as

$$\dot{L}_d = \dot{L}_0(1 + \tau)^{\frac{1}{4q-2p+4}-1}. \quad (18)$$

where  $\dot{L}_0 = \dot{M}_0\sqrt{GMr_0}$  is the initial angular momentum flux. Pringle (1991) showed that this describes the intermediate asymptotic regime of the evolution of a disc with the boundary condition  $\partial(\nu\Sigma r^{1/2})/\partial r = 0$  at  $r = r_{\text{in}}$  which allows no mass flux out of the disc from the inner boundary (see Eqn.(8)). Pringle (1981) mentioned that this solution could describe the propeller regime (Illarionov & Sunyaev 1975) of a disc in which the centrifugal barrier set by a rapidly rotating magnetosphere prohibits accretion. In this solution radial profile is  $\sigma \propto R^{-(p+1/2)/(q+1)}$  which, again, extends to the origin and blows up. This also is the radial profile in the steady-state counterpart (Sunyaev & Shakura 1977) as shown in the next section. The torque given in Equation (7) consists of two parts, a material and a viscous torque. As there is no matter flux out of the disc, in this solution, the angular momentum flux above is due to the viscous torque only. In order to take up the angular momentum transferred to the disc by this torque, the outer radius of the disc expands more rapidly in this solution than it does in the full accretor solution (see Figure 1).

### 3 AN APPROXIMATE SOLUTION WITH GENERAL BOUNDARY CONDITIONS

The Pringle solutions correspond to two extreme stages: either *all* matter reaching the inner radius of the disc accretes while the angular momentum of the disc is constant (first solution) or *none* accretes (mass of the disc is constant) while the angular momentum of the disc increases with the viscous torque from the inner boundary (second solution).

It would be desirable to have a solution which could accommodate the continuous range of  $\dot{L}/\dot{M}$ . In the linear case ( $q = 0$ ) such a solution can be constructed by superposing the solutions; namely one can multiply the solutions with appropriate constants and adds them up. In the nonlinear case superposition can not be applied.

The heat equation  $\partial_t u = \partial_x \chi \partial_x u$  with power-law heat conduction coefficient ( $\chi = \chi_0 u^q$ ) is mathematically a special case (obtained for  $2p = 3q$ ) of the diffusion equation describing the evolution of the disc. There are self-similar solutions describing the evolution of temperature on a semi-infinite rod  $x = [0, \infty)$  (Zel'Dovich & Raizer 1967) which are then special cases of the Pringle solutions. The first solution is a special case of the full accretion solution and accommodates  $u = 0$  at  $x = 0$  and so all heat inflowing there is absorbed. The other solution is a special case of the full propeller solution and accommodates  $\partial u/\partial x = 0$  at  $x = 0$  which allows no heat flux through the inner boundary (perfect insulator). Recently, (Ekşi 2009) constructed an approximate self-similar solution for the partial insulator boundary condition at  $x = 0$ . In this section we are going to employ the same prescription to the Pringle solutions to obtain an approximate solution for the partial accretion case.

#### 3.1 Solutions in terms of fluxes

As a first step, we write the first and second solutions in terms of mass and angular momentum flux, respectively. It is possible to write the first solution given in Equation (12) in terms of the dimensionless mass flux  $\dot{m} \equiv \dot{M}/\dot{M}_0 = (1 + \tau)^{-1 - \frac{1}{5q-2p+4}}$  as

$$\sigma = \begin{cases} (R^{-p}\dot{m})^{\frac{1}{q+1}} \left[ 1 - k_{p,q} \frac{R^{2-p}}{1+\tau} (R^{-p}\dot{m})^{\frac{1}{q+1}-1} \right]^{1/q}, & \text{if } q \neq 0, \\ (R^{-p}\dot{m}) \exp\left(-\frac{R^{2-p}}{4(p-2)^2(1+\tau)}\right), & \text{if } q = 0 \end{cases} \quad (19)$$

The second solution given in Equation (14), in terms of dimensionless angular momentum flux  $\dot{\ell} \equiv \dot{L}/\dot{L}_0 = (1 + \tau)^{\frac{1}{4q-2p+4}-1}$ , can be written as

$$\sigma = \begin{cases} \left[ R^{-p}(-\dot{\ell}R^{-1/2}) \right]^{\frac{1}{q+1}} \left[ 1 - k_{p,q} \frac{R^{2-p}}{1+\tau} \left( R^{-p}(-\dot{\ell}R^{-1/2}) \right)^{\frac{1}{q+1}-1} \right]^{1/q}, & \text{if } q \neq 0, \\ \left[ R^{-p}(-\dot{\ell}R^{-1/2}) \right] \exp\left(-\frac{R^{2-p}}{4(p-2)^2(1+\tau)}\right), & \text{if } q = 0 \end{cases} \quad (20)$$

Note that the viscous torque is negative when this solution is valid so that  $-\dot{\ell}$  is actually positive.

We have eliminated *most* occurrences of  $\tau$  in favor of mass flux in the full accretor solution and angular momentum flux in the full propeller solution. Note the ‘‘dual form’’ of the solutions ( $\dot{m} \rightarrow -\dot{\ell}R^{-1/2}$ ) which would not exist if we insisted in eliminating *all* occurrences of  $\tau$  in favor of  $\dot{m}$  and  $\dot{\ell}$ , respectively. This leads to another useful property: *The solutions as they are given in Equations (19) and (20) satisfy the diffusion equation (11) even when  $\dot{m}$  and  $\dot{\ell}$  are defined as*

$$\dot{m} = \dot{m}_0(1 + \tau)^{-\mu}, \quad \mu = 1 + \frac{1}{5q - 2p + 4} \quad (21)$$

and

$$\dot{\ell} = \dot{\ell}_0(1 + \tau)^{-\lambda}, \quad \lambda = 1 - \frac{1}{4q - 2p + 4} \quad (22)$$

*i.e. when they are multiplied by some arbitrary constants  $\dot{m}_0$  and  $\dot{\ell}_0$ . This, in the linear cases ( $q = 0$ ), is equivalent to*

multiplying the solution itself with a constant as the flux is then a multiplier of the solution. This property, indispensable for the superposition procedure, would not be valid if we insisted in eliminating all occurrences of  $\tau$  in favor of the fluxes.

### 3.2 Comparing with the steady state solution

The steady-state solution of  $\Sigma$  can be found from Equations (1) and (10). In dimensionless form this reads

$$\sigma = \left[ R^{-p} \left( \dot{m} - \dot{\ell} R^{-1/2} \right) \right]^{\frac{1}{q+1}}. \quad (23)$$

Here  $\dot{m}$  and  $\dot{\ell}$  are integration constants. The solutions in terms of fluxes, given in equations (19) and (20), are equivalent to the original solutions given in Equations (12) and (14), respectively. The meaning of the self-similar solutions when written in the latter form is much transparent showing clearly that the self-similar solutions are special solutions in the sense that they each have a single integration constant (in space) whereas any ratio between  $\dot{m}$  and  $\dot{\ell}$  is possible in the steady state solution given in Equation (23). The steady state counterparts of the solutions given in Equations (19) and (20) would be  $\sigma = [R^{-p}(\dot{m})]^{1/(q+1)}$  and  $\sigma = [R^{-p}(-\dot{\ell}R^{-1/2})]^{1/(q+1)}$ , respectively. The first of these is the full accretor solution with no viscous torque and inner radius at the origin. The other limiting case,  $\sigma = [R^{-p}(-\dot{\ell}R^{-1/2})]^{1/(q+1)}$ , obtained for  $\dot{m} = 0$  from Equation (23), is known as the “dead disc” solution of Sunyaev & Shakura (1977). Such a disc is expected to form in the propeller regime (Illarionov & Sunyaev 1975) though it would not be steady.

### 3.3 Nonlinear “superposition”

The idea of going back from the limiting cases, to the general solution given in Equation (23) suggests a “superposition” principle

$$\left. \begin{aligned} \sigma &= \left[ R^{-p} \left( \dot{m} \right) \right]^{1/(q+1)} \\ \sigma &= \left[ R^{-p} \left( -\dot{\ell} R^{-1/2} \right) \right]^{1/(q+1)} \end{aligned} \right\} \implies \sigma = \left[ R^{-p} \left( \dot{m} - \dot{\ell} R^{-1/2} \right) \right]^{1/(q+1)} \quad (24)$$

which reduces to ordinary summation in the linearity limit ( $q = 0$ ). Using this procedure, the solutions given in Equations (19) and (20) can be “superposed” as

$$\sigma = \begin{cases} \left[ R^{-p} (\dot{m} - \dot{\ell} R^{-1/2}) \right]^{\frac{1}{q+1}} \left[ 1 - k_{p,q} \frac{R^{2-p}}{1+\tau} \left( R^{-p} (\dot{m} - \dot{\ell} R^{-1/2}) \right)^{\frac{1}{q+1}-1} \right]^{1/q}, & \text{if } q \neq 0, \\ \left[ R^{-p} (\dot{m} - \dot{\ell} R^{-1/2}) \right] \exp \left( -\frac{R^{2-p}}{4(p-2)^2(1+\tau)} \right), & \text{if } q = 0. \end{cases} \quad (25)$$

Clearly,  $\dot{\ell}_0 = 0$  case will give the “full accretor” and  $\dot{m}_0 = 0$  will give the “full propeller” solution given in Equations (19) and (20), respectively.

If we plug in the expression given in Equation (25) into the diffusion equation (11) we find that the condition for satisfying it reduces to

$$\frac{1}{q+1} (1+\tau)^{-1} f(R, \tau) \left[ \left( \frac{\ddot{m}(1+\tau)}{\dot{m}} + \mu \right) R^2 \dot{m}^2 + \left( \frac{\ddot{m}(1+\tau)}{\dot{m}} + \frac{\ddot{\ell}(1+\tau)}{\dot{\ell}} + 2 \right) R \dot{m} \dot{\ell} + \left( \frac{\ddot{\ell}(1+\tau)}{\dot{\ell}} + \lambda \right) \dot{\ell}^2 \right] = 0. \quad (26)$$

where  $f(R, \tau)$  is some complicated function not very important for our discussion. The first and the third terms in square brackets vanish upon using Equations (21) and (22), respectively. The second term does not vanish and the condition for Equation (25) to satisfy the diffusion equation (11) reduces to

$$\frac{k_{p,q}}{q+1} \frac{\dot{m} \dot{\ell}}{1+\tau} R f(R, \tau) = 0 \quad (27)$$

where we have used  $2 - \mu - \lambda \equiv k_{p,q}$ . Thus, the expression given in Equation (25) is not an exact solution unless  $\dot{m}_0 = 0$  or  $\dot{\ell}_0 = 0$  (reducing to one of the already known solutions given in Equations (19) and (20), respectively), or when  $k_{p,q} = 0$  which is accomplished when  $q = 0$  i.e. the linearity limit. It thus appears that we have not gained much with the unified expression given in Equation (25) as it is an exact solution only in the already known cases. Yet, we will show in the following that the unified expression given in Equation (25) not only illuminates the meaning and complementarity of the known solutions but also motivates a very accurate approximate solution describing the partial accretion regime becoming exact for  $\tau \rightarrow \infty$ , practically achieved in a few viscous time-scales.

### 3.4 Why not an exact solution?

Could there be an exact solution of the diffusion equation which could accommodate boundary conditions in which angular momentum flux per unit mass accretion rate could take any value? In order that a self-similar solution is found no scale should exist in the problem (Barenblatt 1996). The expression given in Equation (25) or any expression with both mass accretion

rate and angular momentum flux having finite values can not be an exact solution because of the presence of the length scale  $l = \Sigma(0)/\Sigma'(0) \propto (\dot{L}/\dot{M})^2/GM$  creeping into the problem through the boundary condition and destroying the very condition for the existence of a self-similar solution. Accordingly, the exact solutions given in Equations (19) and (20) are found either when  $l = 0$  ( $\dot{L} = 0$ ) or when  $l \rightarrow \infty$  ( $\dot{M} = 0$ ). Any attempt to find a solution with a finite inner radius also would suffer from the same problem as this also would introduce a length scale into the problem (Spruit & Taam 2001) except for the case  $2p = 3q$  where the equation is symmetric under translations so that the origin can be shifted. We stress that a solution obtained by the non-linear superposition of self-similar solutions is not equivalent to shifting the origin of the coordinates.

The superposition procedure in the linear case also introduces a length scale into the problem. Yet the superposed expression ( $q = 0$  case in Equation (25)) is an exact solution. The presence of a scale does not hinder the exact solution in the linear case because, as hinted in Equation (27), the length scale is coupled to the “non-linearity parameter”  $q$ : vanishing of either renders the expression given in Equation (25) exact.

### 3.5 A more useful “solution”

Note that  $\dot{m}$  and  $\dot{\ell}$  have different time dependencies, as given by Equations (21) and (22), respectively. This implies the inner radius of the disc in the “solution” given in Equation (25) is time-dependent. Note, however, that the generalization to the expression given in Equation (25) is attained from solutions with zero inner radius. For example, the solution with no viscous torque but finite inner radius would be

$$\sigma = \left[ R^{-p} \dot{m} \left( 1 - (R_{\text{in}}/R)^{1/2} \right) \right]^{\frac{1}{q+1}} \quad (28)$$

where  $R_{\text{in}} = r_{\text{in}}/r_0$  (Pringle 1981), rather than  $\sigma = [R^{-p} \dot{m}]^{\frac{1}{q+1}}$ . In order to accommodate cases with finite angular momentum flux we refer to Equation (2) defining the dimensionless torque  $\beta$ . This in dimensionless form can be written as

$$\dot{\ell} \equiv \beta \dot{m} \sqrt{R_{\text{in}}} \quad (29)$$

(recall Eqn. (2)), and write the “solution” given in Equation (25) in the form

$$\sigma = \begin{cases} \left[ R^{-p} \dot{m} (1 - \beta (R_{\text{in}}/R)^{1/2}) \right]^{\frac{1}{q+1}} \left[ 1 - k_{p,q} \frac{R^{2-p}}{1+\tau} \left( R^{-p} \dot{m} (1 - \beta (R_{\text{in}}/R)^{1/2}) \right)^{\frac{1}{q+1} - 1} \right]^{1/q}, & \text{if } q \neq 0, \\ \left[ R^{-p} \dot{m} (1 - \beta (R_{\text{in}}/R)^{1/2}) \right] \exp \left( -\frac{R^{2-p}}{4(p-2)^2(1+\tau)} \right), & \text{if } q = 0 \end{cases} \quad (30)$$

which accommodates the no-viscous-torque inner boundary condition for  $\beta = 1$ . The left panel of Figure 1 shows this *approximate* solution and the exact Pringle solution given in Equation (19) together with the numerical solution obtained with the boundary condition  $\nu \Sigma(r_{\text{in}}, t) = 0$ .

The numerical solution (see the next section for the details of the numerical method) is started from a Gaussian initial profile. In comparing the solutions we have calculated the mass and angular momentum in this Gaussian surface density distribution and used these values for the analytical solution. No fitting procedure is applied. As first shown by Cannizzo et al. (1990) and Pringle (1991) the figures demonstrate that once the initial conditions are forgotten in a few viscous timescales, the evolution of the disc proceeds self-similarly. It is instructive to compare the exact Pringle solution given in Equation (19) and the approximate solution given in Equation (30): The approximate solution describes the inner region of the disc much better though they are both satisfactory for the intermediate and outer regions. The mass flow rate in the numerical and analytical solutions, however, are the same (see for example the right panel of Figure 1 in Ertan et al. (2009)). In reality, in order that all inflowing mass accretes, the boundary condition  $\Sigma(r_{\text{in}}, t) = 0$  must be satisfied. The exact self-similar solution overestimates the surface mass density near the inner region such that this extra matter at the inner region compensates the reduction in the mass flow rate due to reduced density gradient. The right panel of Figure 1 stands for the full propeller solution. In this case we see that the exact solution given in Equation (20) does very fine except that it extends to the origin though real discs have finite radius. The outer radius of the disc, in order to take up the angular momentum imparted from the inner boundary, moves out more rapidly in this case.

The radial profile of the full propeller solution given in Equation (20),  $\sigma \propto R^{-(p+1/2)/(q+1)}$ , is steeper than the radial profile of the full accretor solution given in Equation (19),  $\sigma \propto R^{-p/(q+1)}$  (Spruit & Taam 1993). This leads to enhanced accretion in transitions from the propeller to the accreting regimes. This then will lead to the inwards movement of the inner disc radius  $r_{\text{in}}$  leading to cyclic behavior in systems at the brink of transitions between accretor and propeller regimes (Spruit & Taam 1993; D’Angelo & Spruit 2012).

## 4 RESULTS: A SOLUTION FOR PARTIAL ACCRETION

In this section we demonstrate that the approximate solution given in Equation (30) describes discs with partial accretion accurately.

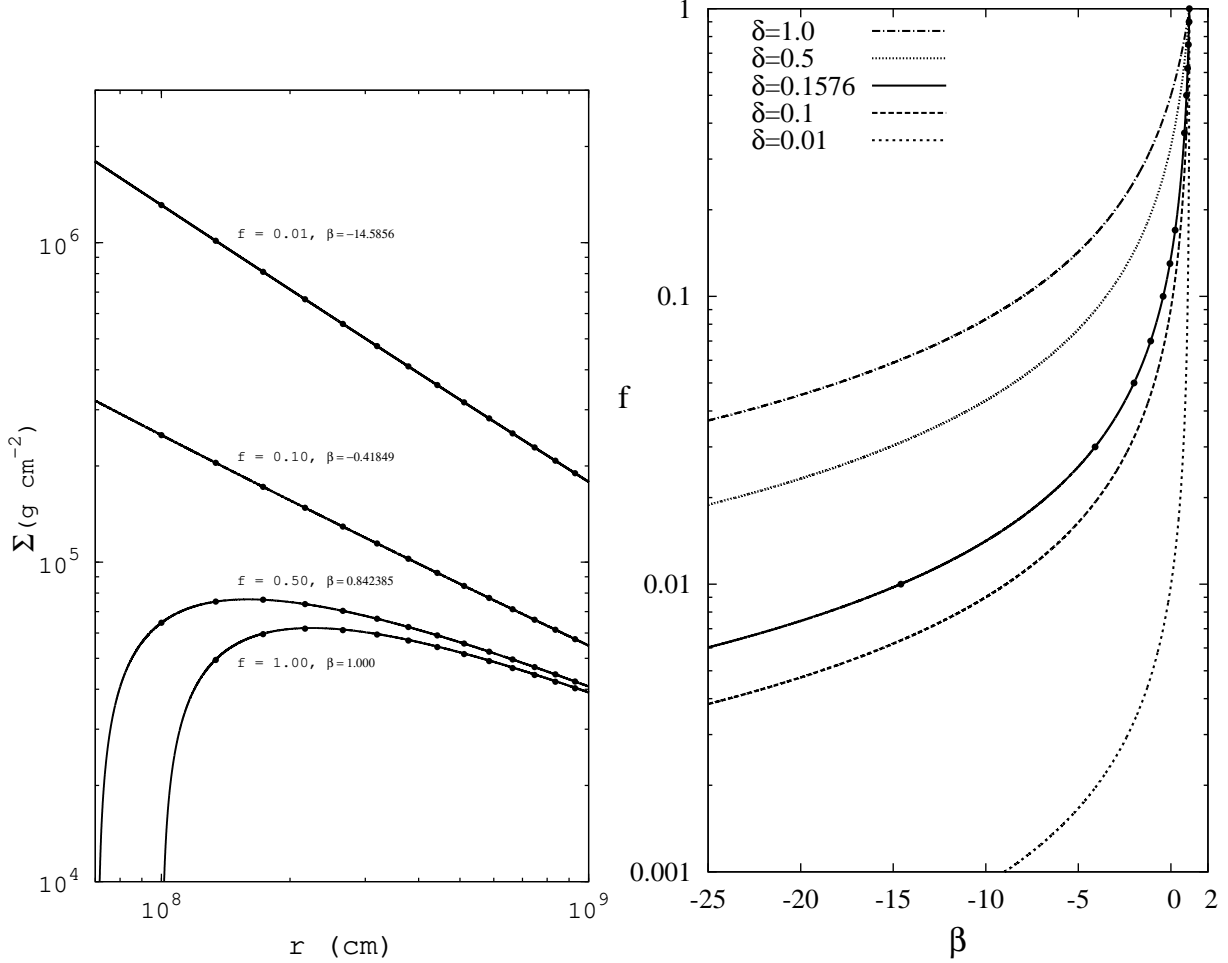


**Figure 2.** The left panel shows the surface mass density profile for discs with partial accretion. The cases for  $f = 0.01, 0.1, 0.5$  and  $1$  are shown. The right panel shows the relation between the fraction of mass flux,  $f$ , that traverses the inner boundary of the disc and the dimensionless torque at the inner boundary,  $\beta$  as given in Equation (40). The data points are the  $\beta$  values obtained by fitting the surface mass density given in Equation (30) to the numerical solution for a value of  $f$ . In the Figure we have not applied any fitting procedure, but used  $\delta \equiv \Delta x/x_{\text{in}} = 0.1576$  from our simulation parameters.

#### 4.1 Numerical Method

In solving the diffusion equation (9) numerically we first transform to the “specific angular momentum coordinate”  $x \equiv r^{1/2}$  and use  $S \equiv x\Sigma$  (Bath & Pringle 1981). The equation becomes

$$\frac{\partial S}{\partial t} = \frac{1}{x^2} \frac{\partial^2}{\partial x^2} (\nu S). \quad (31)$$

where  $\nu = Cx^{2p-q}S^q$ . With this notation Equation (8) becomes

$$\dot{M} = 3\pi \frac{\partial}{\partial x} (\nu S). \quad (32)$$

These equations are discretized and the new value of  $S$  at each grid point is found by

$$S_i^{\text{new}} = S_i + \frac{\Delta t}{(x_i \Delta x)^2} [(\nu S)_{i+1} + (\nu S)_{i-1} - 2(\nu S)_i]. \quad (33)$$

The discretization of Eqn. (32) gives accretion rate at each grid point as

$$\dot{M}_i = 3\pi \frac{(\nu S)_{i+1} - (\nu S)_i}{\Delta x}. \quad (34)$$

We have used  $i_{\text{max}} = 2000$  grids  $x_i = x_0 + i\Delta x$  where  $x_0 = r_0^{1/2}$ . We have taken  $r_0 = 10^8$  cm and  $r_{i_{\text{max}}} = 10^{13}$  cm.

#### 4.2 Inner Boundary Condition for Partial Accretion

The mass flux at the inner boundary of the disc ( $i = 0$ ) is

$$\dot{M}_* = 3\pi \frac{(\nu S)_1 - (\nu S)_0}{\Delta x} \quad (35)$$

Accordingly, the maximum mass flux is obtained for  $(\nu S)_0 = 0$ , the full accretor boundary condition, as

$$\dot{M}_{\max} = 3\pi \frac{(\nu S)_1}{\Delta x}. \quad (36)$$

We have used the boundary condition  $(\nu S)_0 = 0$  for the full accretion regime (see left panel in Figure 1).

According to Equation (35) again,  $\dot{M}_* = 0$  if  $(\nu S)_0 = (\nu S)_1$  and we have employed this boundary condition for the full propeller regime (see right panel in Figure 1). If a fraction  $f$  of  $\dot{M}_{\max}$  accretes

$$f\dot{M}_{\max} = 3\pi \frac{(\nu S)_1 - (\nu S)_0}{\Delta x} \quad (37)$$

is satisfied which implies

$$(\nu S)_0 = (1 - f)(\nu S)_1. \quad (38)$$

In the following, we employ this boundary condition for simulating the evolution of discs in which a fraction  $f$  of the inflowing mass flux traverses the inner boundary and the rest  $1 - f$  remains in the disc. Note that  $f = 1$  and  $f = 0$  cases correspond to the well know full accretor and full propeller boundary conditions, respectively.

With  $x = r^{1/2}$  and  $S = \Sigma x$  Equation (3) can be written as

$$\nu S = \frac{\dot{M}}{3\pi}(x - \beta x_{\text{in}}) \quad (39)$$

Finding  $(\nu S)_0$  and  $(\nu S)_1$  from this equation and plugging into Equation (38) gives

$$\delta = \frac{1 - \beta}{1 - f} f \quad (40)$$

where

$$\delta \equiv \frac{\Delta x}{x_{\text{in}}} = \frac{\Delta r}{2r_{\text{in}}} \quad (41)$$

which is the relative width of grids in the specific angular momentum space. For our simulation parameters  $\delta = 0.1576$ .

We have performed simulations of disc evolution for a range of  $f$  values from 0.01 to 1 keeping the value of  $f$  constant throughout the simulation. For each value of  $f$  we have seen that the self-similar evolution of the disc is well described by the approximate solution given in Equation (30), for a certain value of  $\beta$  found by solving  $\beta$  from Equation (40):

$$\beta = 1 - \frac{1 - f}{f} \delta. \quad (42)$$

The left panel of Figure 2 shows the surface density profile in the inner region of the disc at  $t = 0.1$  years for  $f = 0.01, 0.10, 0.50$  and  $1.00$ . The corresponding  $\beta$  values are also written in the Figure. The right panel of Figure 2 shows the relation given in Equation (40) together with data points from our numerical simulations. The Figure also shows results for other values of  $\delta$  from 0.01 to 1.

The relative width given in Equation (40) is determined by the number of grids we have chosen. It thus appears as a numerical quantity that would vanish if we could do numerical computing with infinite number of grids. At the inner boundary of the disc the matter rotating with keplerian angular velocity has to come to corotation with the star over some region of narrow width, the boundary layer. In our numerical solution of the diffusion equation (9) in which the Keplerian rotation is built in, non-keplerian rotation in the boundary layer can not be modeled and it is implicitly assumed that this transition takes place at the innermost grid and is unresolved. For real discs which do not have grids,  $\delta$  has the physical meaning as the relative width of the region over which matter in the disc is brought into corotation with the star. Equation (40) then tells that the relative width of this transition region is determined by the fraction of matter that could traverse it and the dimensionless torque. The relative width is determined by the stresses that bring the matter in the disc to co-rotation with the star. It is not necessarily the viscous torques. In the case of magnetized stars truncating the disc beyond the stellar surface this could be the magnetic stress applied by the rotating magnetosphere of the star.

#### 4.3 Partial Accretion Stage Away From Equilibrium

In the previous subsection the value of  $f$  was kept constant throughout the simulation. It was found that the accretion rate leaving the disc  $\dot{M}_*$  follows precisely the value given in Equation (17) calculated from the full accretor solution and not less of it. This is because when a fraction  $f$  of the inflowing mass accretes and the rest  $1 - f$  remains in the disc the surface density  $\Sigma$  and subsequently the accretion rate increases. Within a viscous time-scale in the disc  $\dot{M}_{\max}$  increases so that  $f\dot{M}_{\max} = \dot{M}_d$  and not something less. Self-similar approximate solution given in Equation (30) describes this asymptotic stage.

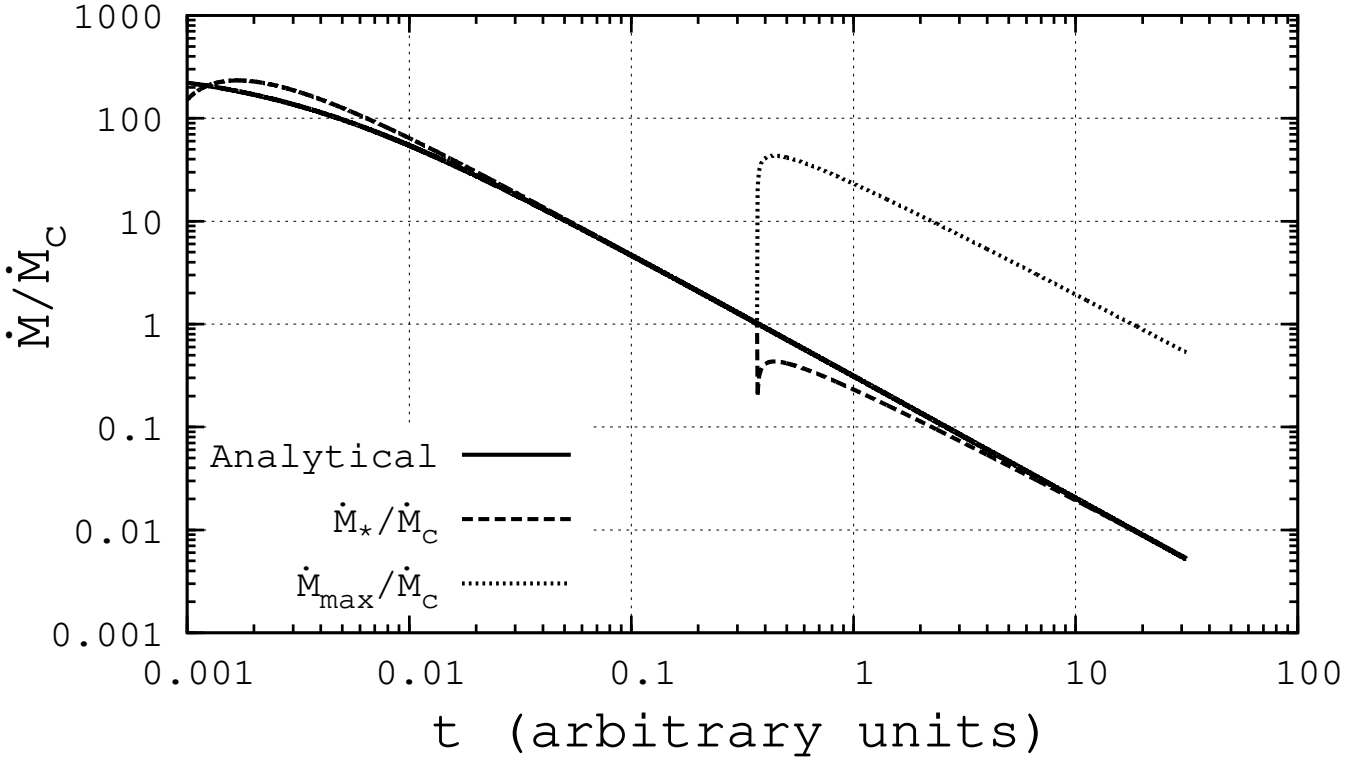


**Figure 3.** Mass accretion rate in units of critical mass flow rate  $\dot{M}_c$  at which partial accretion starts. The solid line shows the analytical expression of mass accretion rate given in Equation (17). Initially  $\dot{M} > \dot{M}_c$  and so all mass accretes ( $f = 1$ ). The dashed lines showing  $\dot{M}_{\max}$  (see Eqn.(36)) and dotted lines showing  $\dot{M}_*$  in units of  $\dot{M}_c$  coincide at this stage and they both catch up with the analytical expression soon after the initial conditions are forgotten. When the mass inflow rate drops below  $\dot{M}_c$  only a fraction  $f = 0.01$  is allowed to accrete onto the central object using the boundary condition given in Equation (38). Although  $\dot{M}_*$  initially drops abruptly as a result of this boundary condition, it catches up with the analytical value given in Equation (17) in a viscous time-scale. This is because the density at the inner disc increases in response as 99% of the inflowing mass is retained in the disc i.e.  $\dot{M}_{\max}$  tends to increase to  $\dot{M}_d/f$  so that its multiplication with  $f$  still gives  $\dot{M}_d$ .

In order to see the behavior of the system when the boundary condition changes we should change the boundary condition more rapidly than the viscous time-scale in the disc. With this motivation we have changed  $f$  from 1 to 0.01 abruptly at a critical mass flow rate  $\dot{M}_c$  at which centrifugal barrier sets in. In real systems, of course, we expect that  $f$  will change more smoothly with the fastness parameter (see e.g. Ekşi & Kutlu 2010). The result of this simulation is shown in Figure 3. We observe that with the start of the partial accretion regime the accretion rate onto the star deviates from its trend given by Equation (17). This is only for a brief epoch because the rest of the matter retained in the disc increases  $\dot{M}_{\max}$  to  $\dot{M}_d/f$  so that  $\dot{M}_* = f\dot{M}_{\max}$  asymptotes to the value given by Equation (17). The transient stage following the immediate aftermath of the transition to partial accretion is not modeled by the approximate self-similar solution given in Equation (30) as self-similar solutions describe the asymptotic stage when the system reaches quasi-equilibrium.

## 5 DISCUSSION

By using a recently suggested prescription we have constructed an approximate self-similar solution, given in Equation (25), describing the evolution of a partially accreting disc. This motivated another approximate solution given in Equation (30) which has a constant finite inner radius. We have numerically shown that this solution describes the asymptotic stage achieved after a few viscous time-scales just like the exact solutions but describes the continuous range of inner boundary conditions between full accretion and full propeller. The approximate solution describes the inner region of the disc even better than the exact solution in the full accretion stage ( $f = 1$ ).

The partial accretion might lead to a rapid decline stage (Ibragimov & Poutanen 2009) during an outburst of a neutron star soft X-ray transient when the accretion rate drops below a critical value at which the inner radius moves beyond the corotation radius and the centrifugal barrier allows only a fraction of the inflowing matter from the off midplane of the disc (Ekşi & Kutlu 2010). Our results imply that partial accretion stage can change the accretion luminosity only if the decay timescale is short so that the inner boundary condition changes abruptly. Otherwise the mass accumulation at the inner boundary increases the accretion rate onto the central object to the same value it would have if there was no partial accretion

within the viscous time-scale. As the viscous time scale in the disc increases with the size of the disc it leads to the expectation that partial accretion can lead to a rapid decline stage in systems allowing small size discs i.e. transient systems with short orbital periods like accreting millisecond pulsars.

The self-similar solutions considered here are more appropriate for free discs e.g. supernova debris discs around young neutron stars (Michel & Dessler 1981; Alpar 2001; Chatterjee et al. 2000) rather than the tidally truncated discs in binary systems. A debris disc was discovered by Wang et al. (2006) around an anomalous X-ray pulsar (AXP; see Mereghetti (2008) for a review). Central compact objects (see de Luca 2008, for a review) like Cas A might also harbor fallback discs (Alpar 2001). Tagieva et al. (2003) mentioned that fallback disc models of AXPs should incorporate accretion and propeller mechanisms working simultaneously. Partial accretion was proposed by Ekşi & Alpar (2003) to explain the present day luminosities of AXPs if they have descended from 10 ms spin periods by interacting with fallback discs. Our results imply for these systems that even if some of these systems are in a partial accretion regime, their long term luminosity trend is determined by the mass flow rate derived from the full accretion solution of Pringle (1974). Mass flow rate variations due to disc instabilities would result in modifications of this accretion rate if these changes occur sufficiently rapid.

## REFERENCES

- Alpar M. A., 2001, *ApJ*, 554, 1245  
 Barenblatt G. I., 1996, *Scaling, Self-similarity, and Intermediate Asymptotics*  
 Bath G. T., Pringle J. E., 1981, *MNRAS*, 194, 967  
 Cannizzo J. K., Lee H. M., Goodman J., 1990, *ApJ*, 351, 38  
 Chan C.-k., Psaltis D., Özel F., 2005, *ApJ*, 628, 353  
 Chatterjee P., Hernquist L., Narayan R., 2000, *ApJ*, 534, 373  
 D’Angelo C. R., Spruit H. C., 2011, *MNRAS*, 416, 893  
 D’Angelo C. R., Spruit H. C., 2012, *MNRAS*, 420, 416  
 de Luca A., 2008, in C. Bassa, Z. Wang, A. Cumming, & V. M. Kaspi ed., *40 Years of Pulsars: Millisecond Pulsars, Magnetars and More* Vol. 983 of American Institute of Physics Conference Series, Central Compact Objects in Supernova Remnants. pp 311–319  
 Ekşi K. Y., 2009, *ArXiv e-prints*: 0908.3337  
 Ekşi K. Y., Alpar M. A., 2003, *ApJ*, 599, 450  
 Ekşi K. Y., Kutlu E., 2010, *ArXiv e-prints*: 1010.1528  
 Ertan Ü., Ekşi K. Y., Erkut M. H., Alpar M. A., 2009, *ApJ*, 702, 1309  
 Frank J., King A., Raine D. J., 2002, *Accretion Power in Astrophysics: Third Edition*  
 Ibragimov A., Poutanen J., 2009, *MNRAS*, 400, 492  
 Illarionov A. F., Sunyaev R. A., 1975, *A&A*, 39, 185  
 Lynden-Bell D., Pringle J. E., 1974, *MNRAS*, 168, 603  
 Menou K., Esin A. A., Narayan R., Garcia M. R., Lasota J.-P., McClintock J. E., 1999, *ApJ*, 520, 276  
 Mereghetti S., 2008, *A&ARv*, 15, 225  
 Michel F. C., Dessler A. J., 1981, *ApJ*, 251, 654  
 Mineshige S., 1991, *MNRAS*, 250, 253  
 Mineshige S., Nomoto K., Shigeyama T., 1993, *A&A*, 267, 95  
 Perna R., Hernquist L., Narayan R., 2000, *ApJ*, 541, 344  
 Pringle J. E., 1974, *PhD thesis*, Univ. Cambridge, (1974)  
 Pringle J. E., 1981, *ARAA*, 19, 137  
 Pringle J. E., 1991, *MNRAS*, 248, 754  
 Pringle J. E., Rees M. J., 1972, *A&A*, 21, 1  
 Romanova M. M., Ustyugova G. V., Koldoba A. V., Lovelace R. V. E., 2004, *ApJ*, 616, L151  
 Shakura N. I., Sunyaev R. A., 1973, *A&A*, 24, 337  
 Spruit H. C., Taam R. E., 1993, *ApJ*, 402, 593  
 Spruit H. C., Taam R. E., 2001, *ApJ*, 548, 900  
 Sunyaev R. A., Shakura N. I., 1977, *Pis ma Astronomicheskii Zhurnal*, 3, 262  
 Tagieva S. O., Yazgan E., Anay A., 2003, *International Journal of Modern Physics D*, 12, 825  
 Tanaka T., 2011, *MNRAS*, 410, 1007  
 Ustyugova G. V., Koldoba A. V., Romanova M. M., Lovelace R. V. E., 2006, *ApJ*, 646, 304  
 Wang Z., Chakrabarty D., Kaplan D. L., 2006, *Nature*, 440, 772  
 Zel’Dovich Y. B., Raizer Y. P., 1967, *Physics of shock waves and high-temperature hydrodynamic phenomena*